Int J Clin Exp Pathol 2017;10(2):1549-1557
www.ijcep.com /ISSN:1936-2625/IJCEP0029150

Original Article

Expression of 78 kD glucose-regulated protein is increased in cirrhotic cardiomyopathy induced by intestinal endotoxin

Minli Lv[1], Huiying Zhang[2], Lili Zhang[2], Jianhong Guo[3], Jiantao Jia[2], Xiaoxia Tian[2], Jingquan Ji[2], Baohong Li[2], Dewu Han[3], Cheng Ji[4]

[1]ICU of The Second Hospital of Shanxi Medical University, Taiyuan, Shanxi, China; [2]Department of Pathophysiology, Changzhi Medical College, Changzhi, Shanxi, China; [3]Institute of Hepatology, Shanxi Medical University, Taiyuan, Shanxi, China; [4]USC Research Center for Liver Disease, Department of Medicine, Keck School of Medicine, University of Southern California, Los Angeles, CA, United States

Received March 25, 2016; Accepted May 28, 2016; Epub February 1, 2017; Published February 15, 2017

Abstract: Aims: This study is to investigate the role of 78 kD glucose-regulated protein (GRP78) in cardiomyopathy induced by intestinal endotoxin in a rat model of liver cirrhosis. Methods: The liver cirrhosis model was established by challenging rats with carbon tetrachloride, lard and alcohol. A total of 51 male SD rats were randomly divided into liver cirrhosis group (n = 33) and control group (n = 18). Measurements were conducted at week 4, week 6 and week 8 of the liver cirrhosis modeling. At each time point, 11 rats of the liver cirrhosis group and 6 rats of the control group were used. The cardiac functions were determined at week 8. Levels of tumor necrosis factor-α (TNF-α) and malondialdehyde (MDA) were detected by radioimmunoassay and thiobarbituric acid assay, respectively. The numbers of cardiomyocytes were detected by toluidine blue staining. The contents of collagen were determined by Van Giesan staining. Expression of GRP78 and hypoxia-inducible factor-1α (HIF-1α) was detected by immnunohistochemistry. Results: The systolic and diastolic function of the heart was significantly decreased in the liver cirrhosis group at week 8 compared with that of the control group ($P < 0.05$). The levels of TNF-α, MDA, collagen, GRP78, and HIF-1α expression in myocardial tissues were significantly increased in the liver cirrhosis group compared with those in the control group ($P < 0.05$). The numbers of cardiomyocytes were decreased in the progression of liver cirrhosis ($P < 0.05$). The plasma endotoxin levels were positively correlated with MDA and GRP78 expression levels in myocardial tissues ($P < 0.05$). The expression levels of GRP78 were positively correlated with levels of homocysteine, alanine aminotransferase, MDA, and HIF-1α expression ($P < 0.05$). Conclusion: Expression of 78 kD glucose-regulated protein is increased during myocardial remodeling induced by intestinal endotoxin in the rat model of liver cirrhosis.

Keywords: Liver cirrhosis, endotoxin, 78 kD glucose-regulated protein, myocardial remodeling

Introduction

The 78 kD glucose-regulated protein (GRP78) is a chaperone molecule that is located in the endoplasmic reticulum [1]. In the event of endoplasmic reticulum stress (ER stress), GRP78 plays an important role in the unfolded protein response, reestablishing the balance of endoplasmic reticulum functions, and attenuating the ER stress-induced damages to cells [2]. However, when the sustained and serious ER stress occurs, GRP78 may lead to apoptosis and tissue damages through induction and activation of caspase-12, CHOP, and other pro-apoptotic factors [3] (Xu et al.,).

Due to changes in hepatic functions and the occurrence of intestinal endotoxemia, liver cirrhosis leads to damages in extrahepatic tissues, including the heart, lungs, brain, and kidneys. Clinical studies showed that the left atrial cavity and the left ventricular cavity were expanded in the patients with liver cirrhosis. The walls of left atrium became thinner but the walls of left ventricular became hypertrophy [4-7]. Two dimensional Doppler ultrasound evaluations revealed that the systolic and diastolic functions of heart in the patients with liver cirrhosis were disordered [8]. Intestinal endotoxemia can not only aggravate liver diseases, but also play an important role in the

occurrence and development of various complications of liver cirrhosis [9]. Cirrhotic cardiomyopathy is likely to be induced by intestinal endotoxemia. Cardiomyocytes contain abundant sarcoplasmic reticulum/ER system, in which ER stress can be caused by endotoxin [10, 11]. ER contains a large amount of lipids, which is susceptible to peroxidation. Peroxidized lipid further stimulates ER stress and leads to serious damages of cellular functions [12].

In patients with impaired hepatic functions, methionine metabolism is affected, which results in occurrence of hyperhomocysteine. Excessive alcohol consumption can induce liver fat accumulation, liver damages and hyperhomocysteine. The ER stress response genes are also highly expressed, suggesting that ER stress can be induced by high levels of homocysteine [13]. Malondialdehyde (MDA) is the intermediate product of lipid peroxidation, which can reflect the degree of lipid peroxidation and cell damages.

Liver disease is often complicated by hepatopulmonary syndrome at an earlier time. Hypoxia is an important pathological change of the hepatopulmonary syndrome. Hypoxia-inducible factor-1α (HIF-1α) is an important regulatory factor to maintenance of cellular and systemic oxygen homeostasis [14-16]. Previous studies suggested that ER stress played an important role in liver cirrhosis and hepatopulmonary syndrome induced by multiple pathogenic factors. The expression levels of GRP78 were significantly increased in the occurrence of ER stress [10, 17]. The evidence suggests that GRP78 may play a role in cirrhotic cardiomyopathy induced by intestinal endotoxin. In this study, we investigated the effect of GRP78 on cirrhotic cardiomyopathy induced by intestinal endotoxin.

Materials and methods

Reagents

Rabbit anti-rat GRP78 polyclonal antibodies, rabbit anti-HIF-1α polyclonal antibodies and Histostain-Plus Kit (HRP, Broad Spectrum) were purchased from Beijing Biosynthesis Biotechnology Co. Ltd (Beijing, China). Alanine aminotransferase activity assay kit and thiobarbituric acid assay kit for MDA were purchased from Nanjing Jiancheng Bioengineering Institute (Nanjing, China). Limulus Amebocyte Lysate Endotoxin Detection kit was purchased from Xiamen LAL Experimental Factory Co., Ltd (Xiamen, Fujian, China). The radioimmunoassay kit for tumor necrosis factor-α (TNF-α) was purchased from PurevalleyBioteche (Beijing, China). CCl_4 (analytical pure) was purchased from Fuyu Fine Chemical Co., Ltd (Tianjin, China).

Establishment of the liver cirrhosis model

A total of 51 male SD rats, weighed 200 to 240 g, were provided by the Experimental Animal Center of Shanxi Medical School (Taiyuan, Shanxi, China). Experimental animals were randomly divided into the liver cirrhosis group (n = 33) and the control group (n = 18). Liver cirrhosis was established in rat as previously described [18]. Briefly, animals in the liver cirrhosis group were fed with a mixture of maize flour, lard, cholesterol, and alcohol plus subcutaneously injection of CCl_4 oil solution for 8 weeks. The CCl_4 oil solution (400 g/l) was injected at 5 ml/kg body weight at the first day of experiment and at 3 ml/kg body weight from the fourth day on at an interval of three days. Lard was used only in the first two weeks accounting for 20% of the feed. Cholesterol was appended at 0.5% of the feed for the whole experiment. Alcohol was used in the drinking water exclusively (300 ml/l). For control, the animals of the control group had free access to the standard food and water. At week 8 of liver cirrhosis modeling, the cardiac functions were measured. At week 4, week 6 and week 8 of liver cirrhosis modeling, rats were sacrificed by deep anaesthesia and heart tissues were collected for further analysis. At each time point, 11 rats of the liver cirrhosis group and 6 rats of the control group were sacrificed. All animal experiments were conducted according to the ethical guidelines of Changzhi Medical College.

Cardiac function analysis

At week 8 of liver cirrhosis modeling, the cardiac functions were measured. Briefly, a catheter was inserted into the left ventricle via the right common carotid artery. The parameters of left ventricular systolic pressure (LVSP), left ventricular end diastolic pressure (LVEDP), and the maximum rate of change in left ventricular pressure in the isovolumic contraction or relax-

Table 1. Cardiac function of rats in the liver cirrhosis group and the control group (mean ± SD)

Groups	n	LVSP (mmHg)	LVEDP (mmHg)	+ dp/dt max (mmHg/ms)	- dp/dt max (mmHg/ms)
Liver cirrhosis	11	99.13 ± 8.01	18.09 ± 2.81*	5.21 ± 1.07*	2.02 ± 2.30*
Control	6	108.44 ± 7.16	29.71 ± 5.1	8.09 ± 1.81	3.75 ± 1.44

Note: LVSP, left ventricular systolic pressure; LVEDP, left ventricular end diastolic pressure; + dp/dt max, the maximum rate of change in left ventricular pressure in the isovolumic contraction period; - dp/dt max, the maximum rate of change in left ventricular pressure in isovolumicrelaxation period. *$P < 0.05$ vs. control group.

ation period (± dp/dt max) were detected by the BL-420 Data Acquisition & Analysis System (Chengdu Tme Technology Co, Ltd, Chengdu, China).

Thiobarbituric acid assay and radioimmunoassay

Levels of TNF-α and MDA in heart tissue were detected with radioimmunoassay kit and thiobarbituric acid assay kit, respectively. The assays were performed according to the manufacturers' instructions. Protein quantification was determined by the coomassie brilliant blue method.

Van Giesan staining and collagen volume fraction (CVF) determination

Heart tissues were rapidly frozen by liquid nitrogen. After being fixed in formaldehyde and embedded in paraffin, the embedded heart tissues were cut into sections with a thickness of 4 μM. The sections were dewaxed, hydrated in graded alcohols and stained by Van Gieson. Changes in myocardial interstitial collagen were observed by Image HPIAS-2000 Analysis System (Chengdu Tme Technology Co, Ltd, Chengdu, China). CVF referred to the ratio of the area of collagen relative to the total area of the image. Ten fields at high-magnification were randomly taken and areas of collagen were calculated.

Toluidine blue staining

The sections of heart tissues were prepared as above mentioned. The sections were stained by toluidine blue for 20 min, and dehydrated to be transparent. The numbers of cardiomyocytes were observed and counted by an optical microscope (Olympus BX51, Olympus, Tokyo, Japan). Ten fields at high-magnification (× 400) were randomly taken from every section and the average numbers of cardiomyocytes were calculated.

Immunohistochemical staining

The sections of heart tissues were prepared as mentioned above. To inactivate endogenous peroxidase, 3% fresh prepared hydrogen peroxide was added and incubated at room temperature for 15 min. After washing with distilled water, the antigen was repaired by citrate buffer (0.01 M, pH 6.0) with microwave heating. The sections were washed with PBS and blocked with serum blocking solution for 20 min. Then the primary rabbit anti-rat GRP78 polyclonal antibodies (dilution, 1:100) or rabbit anti-HIF-1α polyclonal antibodies (dilution, 1:300) were added and incubated at 4°C in the dark overnight. The secondary biotined goat anti rabbit IgG was added for a 20 min incubation at room temperature. After incubation with streptavidin-biotin complex, the sections were developed with 3, 3'-diaminobenzidine tetrahydrochloride-dihydrate chromogenic reagent. Sections were counterstained with haematoxylin. After hydrochloric acid differentiation and dimethylbenzene transparency, he sections were mounted withneutral gum. Cells with brown staining were defined as GRP78-positive or HIF-1α-positive. Ten fields at high-magnification (× 400) were randomly taken from every section and the positive cells were counted. Positive rate referred to the ratio of the positive cell number relative to the total cell number. At least 100 cells were counted.

Statistical analysis

All results were expressed as mean ± standard deviation (SD). All statistical analyses were performed with SPSS version 10.0 for Windows (SPSS Inc., Chicago, IL, USA). LSD-t test was used to analyze comparisons between groups. ANOVA was used to analyze paired data. Pearson correlation analysis was used to analyze the association between GRP78 expression and other main indicators. *P* value less than 0.05 was considered to be significantly different.

Table 2. Levels of TNF-α and MDA in myocardial tissues of rats (mean ± SD)

Time point	TNF-α (μg/l)		MDA (μM)	
	Liver cirrhosis group (n = 11)	Control group (n = 6)	Liver cirrhosis group (n = 11)	Control group (n = 6)
Week 4	0.37 ± 0.45	0.12 ± 0.07	1.73 ± 0.62*	0.42 ± 0.08
Week 6	0.71 ± 0.16*	0.16 ± 0.05	1.94 ± 0.77*,#	0.60 ± 0.06
Week 8	1.23 ± 0.25*,#	0.14 ± 0.08	4.92 ± 2.67*,#,◊	0.68 ± 0.09

Note: *P < 0.05 vs. control group; #P < 0.05 vs. those at week 4; ◊P < 0.05 vs. those at week 6.

Results

The systolic and diastolic function of the heart is affected by liver cirrhosis

To investigate the cardiac functions in rats with liver cirrhosis, cardiac function analysis was performed at week 8 of liver cirrhosis modeling to measure the parameters of LVSP, LVEDP, and ± dp/dt max. As shown in **Table 1**, LVEDP and ± dp/dt max were significantly decreased in the liver cirrhosis group compared with those in the control group ($P < 0.05$). Also, LVSP showed a downward trend in rats with liver cirrhosis compared with control. However, the difference in LVSP between these two groups was not significant. These results indicate that both systolic and diastolic function of the heart can be affected in the liver cirrhosis group.

Levels of TNF-α and MDA in myocardial tissues are significantly increased during the progression of liver cirrhosis

To detect the levels of TNF-α and MDA in myocardial tissues, the radioimmunoassay and thiobarbituric acid assay was performed, respectively. The results were shown in **Table 2**. For levels of TNF-α, at week 4 of liver cirrhosis modeling, there was no significant difference in TNF-α level between liver cirrhosis group and control group. At week 6 and week 8 of liver cirrhosis modeling, TNF-α levels in the liver cirrhosis were significantly higher than those in the control group (week 6, 0.71 ± 0.16 μg/l VS 0.16 ± 0.05 μg/l; week 8, 1.23 ± 0.25 μg/l VS 0.14 ± 0.08 μg/l) ($P < 0.05$). Compared with that at week 4 (0.37 ± 0.45 μg/l), TNF-α level in the liver cirrhosis group at week 8 (1.23 ± 0.25 μg/l) was significantly higher ($P < 0.05$).

The MDA levels in the liver cirrhosis group at week 4, week 6 and week 8 were 1.73 ± 0.62 μM, 1.94 ± 0.77 μM, and 4.92 ± 2.67 μM, respectively. The MDA levels in the control group at week 4, week 6 and week 8 were 0.42 ± 0.08 μM, 0.60 ± 0.06 μM, and 0.68 ± 0.09 μM, respectively. Compared with the corresponding control group, the liver cirrhosis group had significantly higher levels of MDA at week 4, week 6 and week 8 ($P < 0.05$). MDA levels in the liver cirrhosis group at week 6 and week 8 were significantly higher than that at week 4 ($P < 0.05$). MDA level in the liver cirrhosis group at week 8 was significantly higher than that at week 6 ($P < 0.05$). These results indicate that levels of TNF-α and MDA in myocardial tissues are significantly increased during the progression of liver cirrhosis.

The numbers of cardiomyocytes are decreased during the progression of liver cirrhosis

To investigate the effects of liver cirrhosis on the myocardial structures, toluidine blue staining was performed to observe the morphology and numbers of myocardial cells. In the control group, cardiomyocytes showed normal morphology (**Figure 1A**). At week 4 in the liver cirrhosis group, there were spotty pathological changes, mild edema, smaller intercellular spaces, and slightly blurred boundaries in cardiomyocytes (**Figure 1B**). At week 6 in the liver cirrhosis group, cardiomyocytes showed severe edemas and a range of different cell sizes (**Figure 1C**). At week 8 in the liver cirrhosis group, a large area of dissolved necrosis cells, obvious muscle fiber fractures and blurred boundaries were observed in myocardial tissue. In addition, varying degrees of inflammatory cell infiltration were observed from lesion area (**Figure 1D**).

The numbers of cardiomyocytes were counted by BI-2000 Medical image analysis software. The number of cardiomyocytes was 816.76 ± 7.17 in the control group (n = 18). The number of cardiomyocytes in the liver cirrhosis group was 245.41 ± 3.1 at week 4, 113.84 ± 2.77 at week 6, and 40.17 ± 2.67 at week 8, significantly lower than that of the control group ($P < 0.05$). The number of cardiomyocytes in liver cirrhosis group at week 8 was significantly decreased compared with those at week 6 ($P < 0.05$). These results indicate that the number

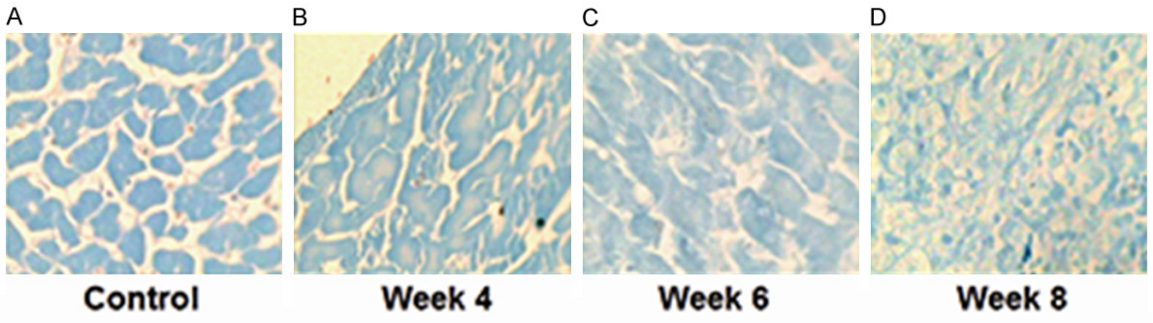

Figure 1. Morphology and numbers of cardiomyocytes in the liver cirrhosis groups and the control group. Toluidine blue staining was performed to observe the morphology and numbers of cardiomyocytes. Morphology and numbers of myocardial cells were visualized by an optical microscope (× 400). Representative staining results were shown. A. Cardiomyocytes in the control group. B. Cardiomyocytes in the liver cirrhosis group at week 4. C. Cardiomyocytes in the liver cirrhosis group at week 6. D. Cardiomyocytes in the liver cirrhosis group at week 8.

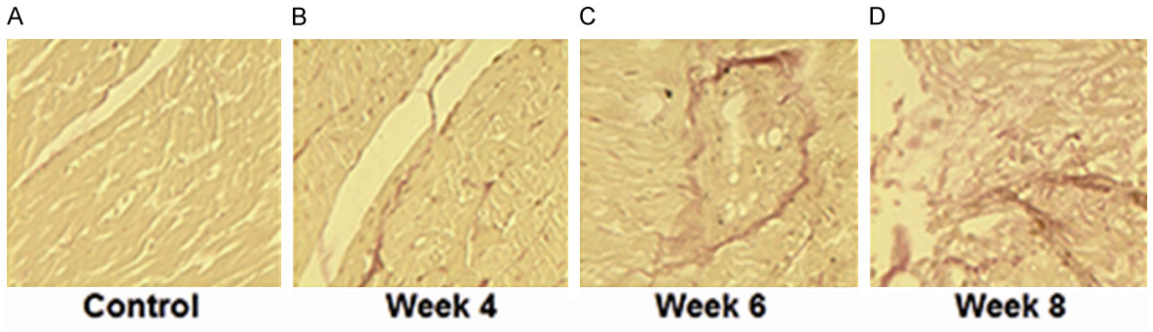

Figure 2. Distribution of myocardial interstitial collagen. Van Giesan staining was performed to observe the distribution of collagen in myocardial tissues. Cardiomyocytes were stained yellow and collagen was stained red. Collagen distributions in myocardial tissues were analyzed by Image HPIAS-2000 Analysis System. Representative staining results were shown. A. Control group. B. The liver cirrhosis group at week 4. C. The liver cirrhosis group at week 6. D. The liver cirrhosis group at week 8.

of cardiomyocytes is decreased during the progression of liver cirrhosis.

The myocardial interstitial collagen is significantly increased in the liver cirrhosis group

To investigate the distribution of myocardial interstitial collagen, Van Giesan staining was performed. As shown in **Figure 2A**, myocardial interstitial collagen in the control group was rarely detectable. For the liver cirrhosis group, small amounts of collagen fibers were stained red at week 4 (**Figure 2B**). The content of interstitial collagen was significantly increased, and the necrotic myocardial cells were surrounded by a large number of disordered crisscross of collagen fibers in the liver cirrhosis group at week 6 (**Figure 2C**). The myocardial collagen fibers were radially distributed in the myocardial necrosis around the foci of myocardial necrosis in the cirrhosis group at week 8 (**Figure 2D**). The CVF value in the control group was 2.11 ± 0.52 (n = 18). CVF values in the liver cirrhosis group at week 4, week 6 and week 8 were 5.83 ± 0.927, 7.47 ± 1.04, and 12.56 ± 2.88, respectively. The CVF values in the liver cirrhosis group at week 4, week 6 and week 8 were significantly increased compared with those in the control group, respectively ($P < 0.05$). Compared with that at week 6, the CVF value in the liver cirrhosis group at week 8 was significantly increased ($P < 0.05$). These results indicate that the myocardial fibrosis occurs in the liver cirrhosis progress.

Expression levels of GRP78 are increased during the progression of liver cirrhosis

To detect the expression of GRP78 in heart tissues, immunohistochemical staining was per-

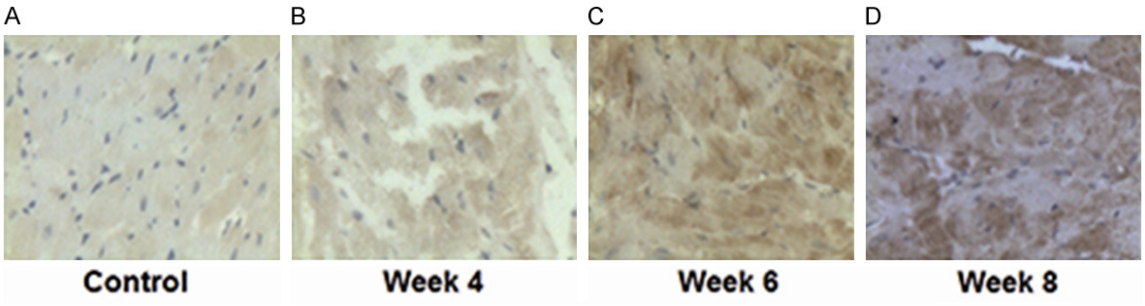

Figure 3. Expression of GRP78 in myocardial tissues. Immunohistochemical staining was performed to investigate the expression of GRP78 in myocardial tissues. Representative immunohistochemical staining results were shown. Cells stained brown were GRP78-positive. The expression of GRP78 in cardiomyocytes was visualized at high magnification (× 400). A. Control group. B. The liver cirrhosis group at week 4. C. The liver cirrhosis group at week 6. D. The liver cirrhosis group at week 8.

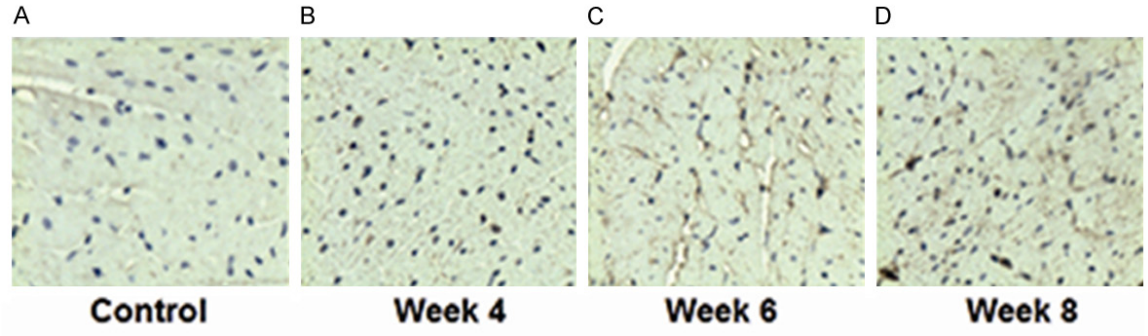

Figure 4. The expression of HIF-1α in myocardial tissues. Immunohistochemical staining was performed to investigate expression of HIF-1α in myocardial tissues. Representative immunohistochemical staining results were shown. Cells stained brown were HIF-1α-positive. The expression of HIF-1α in cardiomyocytes was visualized at high magnification (× 400). A. Control group. B. The liver cirrhosis group at week 4. C. The liver cirrhosis group at week 6. D. The liver cirrhosis group at week 8.

formed. Representative immunohistochemical staining were shown. The positive expression of GRP78 showed as brown granules. As shown in **Figure 3A**, in the control group (n = 18), light brown granules were barely observed. However, visible dense dark brown granules were increased in the cytoplasm of cardiomyocytes in the liver cirrhosis group at week 4, week 6 and week 8 (**Figure 3B-D**). Positive rate of GRP78 expression was 0.031 ± 0.006 in the control group. Positiverates of GRP78 expression were 0.048 ± 0.004 at week 4, 0.070 ± 0.020 at week 6, and 0.080 ± 0.013 at week 8 in the liver cirrhosis group, respectively, significantly higher than those in the control group, respectively ($P < 0.05$). Positive rates of GRP78 expression in the liver cirrhosis group at week 6 and week 8 were significantly increased compared with those at week 4 ($P < 0.05$). These results indicate that the expression levels of GRP78 are increased during liver cirrhosis.

Expression levels of HIF-1α are increased during the progression of liver cirrhosis

To determine the expression level of HIF-1α in the myocardial tissues, immunohistochemical staining was performed. Representative immunohistochemical staining were shown. Cells with brown granules were positive. As shown in **Figure 4A**, in the control group, a small amount of brown granules were evenly distributed in cytoplasm of myocardial cells. However, in the liver cirrhosis group, the brown granules were mainly distributed in the nuclei of myocardial cells, with some surrounding the nuclei. The numbers of dark brown granules were increased in the liver cirrhosis group at week 4, week 6 and week 8 (**Figure 4B-D**). Positive rate of HIF-1α expression in the control group was 0.929 ± 0.171. Positive rates of HIF-1α expression in the liver cirrhosis groupat week 4, week 6 and week 8 were 2.087 ± 0.597, 5.840 ± 0.803,

and 12.31 ± 0.994, respectively. Positive rates of HIF-1α expression in the liver cirrhosis group at week 4, week 6 and week 8 were significantly increased compared with those in the control group ($P < 0.05$). The positive rate of HIF-1α expression in the liver cirrhosis group at week 8 was significantly increased compared with those at week 6 ($P < 0.05$). These results indicate that the expression levels of HIF-1α are increased in the progression of liver cirrhosis.

Expression of GRP78 is positively correlated with other main indicators induced by intestinal endotoxin

To investigate the association between GRP78 expression and other main indicators induced by intestinal endotoxin, Pearson correlation analysis was performed. The plasma endotoxin levels were positively correlated with MDA ($r = 0.768$, $P < 0.05$) and GRP78 expression levels ($r = 0.861$, $P < 0.01$) in myocardial tissues. The expression levels of GRP78 were positively correlated with levels of homocysteine ($r = 0.649$, $p < 0.05$), alanine aminotransferase ($r = 0.691$, $P < 0.05$), MDA ($r = 0.794$, $P < 0.01$), CVF ($r = 0.826$, $P < 0.01$) and HIF-1α expression ($r = 0.618$, $P < 0.05$). These results suggest that GRP78 is an important molecule in the pathogenesis of cardiopathy induced by intestinal endotoxin.

Discussion

In this study, a rat model of liver cirrhosis induced by multiple pathogenic factors was established. Systolic and diastolic dysfunction was observed. Myocardial edema, fatty degeneration, spotty necrosis, decreased cardiaomyocytes and obvious myocardial fibrosis were associated with the liver cirrhosis, which suggests that liver cirrhosis is complicated by the alterations of myocardium.

Intestinal endotoxemia plays an important role in the development of various complications of liver cirrhosis [19-21]. During intestinal endotoxemia, levels of intestinal endotoxin are increased, further stimulating ER stress. Our results showed that the levels of myocardial MDA were significantly increased in the liver cirrhosis group compared with those in the control group, which indicates that lipid peroxidation occurs in myocardial tissues. ER stress caused by oxidative stress or intestinal endotoxin is likely to play an important role in cirrhotic cardiomyopathy. There was hyperhomocysteinemia in the rat model of liver cirrhosis, which may be a cause for the ER stress response associated with cirrhotic cardiomyopathy [22-24].

Hypoxia causes accumulation of lactic acid and acidosis in myocardial tissue, which further induces expression of HIF-1α [25, 26]. In this study, we found that the numbers of myocardial cells were decreased but the content of interstitial collagen was increased in the progression of liver cirrhosis. The expression levels of GRP78 were positively correlated with the expression levels of HIF-1α. These results indicate that hypoxia caused by hepatopulmonary syndrome induces the expression of HIF-1α, which stimulates GRP78 expression to protect cardiomyocytes. However, excessive and prolonged hypoxia may lead to severe ER stress responses with high expression of HIF-1α, which increases apoptosis and damages to cardiomyocytes. In addition, myocardial fibrosis affects blood supply, which also induces the expression of HIF-1α. Thus, hypoxia may be another important factor leading to cirrhotic cardiomyopathy.

Multiple factors are involved in the cirrhotic cardiomyopathy. The decreased cardiomyocytes, interstitial fibrosis, myocardial remodeling, and the gradual declining of cardiac function may be resulted from the liver cirrhosis. Furthermore, liver cirrhosis may induce heart failure and threaten the patient's lives. The expression of GRP78 during the ER stress response plays an important role in myocardial remodeling in the cirrhotic cardiomyopathy.

Acknowledgements

This work was supported by National Natural Science Foundation of China (Grant No, 81070339), International Science and Technology Cooperation Project in Shanxi Province (Grant No, 2010081068), Scientific Research Foundation for Returned Overseas Chinese Scholars in Shanxi Province (Grant No, 211-091) and the Director funding of Key Laboratory of Cellular Physiology co-established by Shanxi Province and Ministry of Education in Shanxi Medical University (Grant No, 2010-09). Cheng Ji is sup-

ported by US NIH grants: R21AA023952 and P30DK048522-22.

Disclosure of conflict of interest

None.

Address correspondence to: Huiying Zhang, Department of Pathophysiology, Changzhi Medical College, 161 Jiefang East Street, Changzhi 046000, Shanxi, China. Tel: +86-136 3355 5266; Fax: +86-355-3034065; E-mail: zhanghy2001@163.com

References

[1] Lee AS. The ER chaperone and signaling regulator GRP78/BiP as a monitor of endoplasmic reticulum stress. Methods 2005; 35: 373-381.
[2] Quinones QJ, de Ridder GG, Pizzo SV. GRP78: a chaperone with diverse roles beyond the endoplasmic reticulum. HistolHistopathol 2008; 23: 1409-1416.
[3] Xu C, Bailly-Maitre B, Reed JC. Endoplasmic reticulum stress: cell life and death decisions. J Clin Invest 2005; 115: 2656-2664.
[4] Fouad YM, Yehia R. Hepato-cardiac disorders. World J Hepatol 2014; 6: 41-54.
[5] Møller S, Bernardi M. Interactions of the heart and the liver. Eur Heart J 2013; 34: 2804-2811.
[6] Sampaio F, Pimenta J, Bettencourt N, Fontes-Carvalho R, Silva AP, Valente J, Bettencourt P, Fraga J, Gama V. Systolic and diastolic dysfunction in cirrhosis: a tissue-Doppler and speckle tracking echocardiography study. Liver Int 2013; 33: 1158-1165.
[7] Wiese S, Hove JD, Bendtsen F, Møller S. Cirrhotic cardiomyopathy: pathogenesis and clinical relevance. Nat Rev Gastroenterol Hepatol 2014; 11: 177-186.
[8] Valeriano V, Funaro S, Lionetti R, Riggio O, Pulcinelli G, Fiore P, Masini A, De Castro S, Merli M. Modification of cardiac function in cirrhotic patients with and without ascites. Am J Gastroenterol 2000; 95: 3200-3205.
[9] Han DW. Intestinal endotoxemia as a pathogenetic mechanism in liver failure. World J Gastroenterol 2002; 8: 961-965.
[10] Ji JQ, Zhang HY, Jia JT, Zhang LL, Chen YX, Wang LM, Tian XX, Feng M, Zhao ZF, Han DW. Role of 78 kD glucose-regulated protein in the development of liver cirrhosis promoted by intestinalendotoxemia in rats. Chinese J Pathophysiol 2010; 26: 2447-2452.
[11] Liu YC, Chang AY, Tsai YC, Chan JY. Differential protection against oxidative stress and nitric oxide overproduction in cardiovascular and pulmonary systems by propofol during endotoxemia. J Biomed Sci 2009; 16: 8.
[12] Martinelli GP, Friedrich VL Jr, Holstein GR. L-citrulline immunostaining identifies nitric oxide production sites within neurons. Neuroscience 2002; 114: 111-122.
[13] Ji C, Kaplowitz N. Betaine decreases hyperhomocysteinemia, endoplasmic reticulum stress, and liver injury in alcohol-fed mice. Gastroenterology 2003; 124: 1488-1499.
[14] Hong WX, Hu MS, Esquivel M, Liang GY, Rennert RC, McArdle A, Paik KJ, Duscher D, Gurtner GC, Lorenz HP, Longaker MT. The Role of Hypoxia-Inducible Factor in Wound Healing. Adv Wound Care 2014; 3: 390-399.
[15] Semenza GL. Oxygen sensing, hypoxia-inducible factors, and disease pathophysiology. Annu Rev Pathol 2014; 9: 47-71.
[16] Semenza GL. Hypoxia-inducible factor 1 and cardiovascular disease. Annu Rev Physiol 2014; 76: 39-56.
[17] Jia JT, Zhang HY, Tian XX, Ji JQ, Zhang LL, Lv ML, Wang MH, Feng M, Zhao ZF, Han DW, Cheng J. Role of 78 kD glucose-regulated protein in development of hepatopulmonary syndrome induced by multiple pathogenic factors. Chinese J Pathophysiol 2011; 27: 1580-1585.
[18] Zhang HY, Han DW, Zhao ZF, Liu MS, Wu YJ, Chen XM, Ji C. Multiple pathogenic factor-induced complications of cirrhosis in rats: a new model of hepatopulmonary syndrome with intestinal endotoxemia. World J Gastroenterol 2007; 13: 3500-3507.
[19] Benjamin J, Singla V, Arora I, Sood S, Joshi YK. Intestinal permeability and complications in liver cirrhosis: A prospective cohort study. Hepatol Res 2013; 43: 200-207.
[20] Jazaeri F, Tavangar SM, Ghazi-Khansari M, Khorramizadeh MR, Mani AR, Dehpour AR. Cirrhosis is associated with development of tolerance to cardiac chronotropic effect of endotoxin in rats. Liver Int 2013; 33: 368-374.
[21] Zhang H, Lv M, Zhao Z, Jia J, Zhang L, Xiao P, Wang L, Li C, Ji J, Tian X, Li X, Fan Y, Lai L, Liu Y, Li B, Zhang C, Liu M, Guo J, Han D, Ji C. Glucose-regulated protein 78 may play a crucial role in promoting the pulmonary microvascular remodeling in a rat model of hepatopulmonary syndrome. Gene 2014; 545: 156-162.
[22] Fernandez A, Matias N, Fucho R, Ribas V, Von Montfort C, Nuño N, Baulies A, Martinez L, Tarrats N, Mari M, Colell A, Morales A, Dubuquoy L, Mathurin P, Bataller R, Caballeria J, Elena M, Balsinde J, Kaplowitz N, Garcia-Ruiz C, Fernandez-Checa JC. ASMase is required for chronic alcohol induced hepatic endoplasmic reticulum stress and mitochondrial cholesterol loading. J Hepatol 2013; 59: 805-813.
[23] Wei HJ, Xu JH, Li MH, Tang JP, Zou W, Zhang P, Wang L, Wang CY, Tang XQ. Hydrogen sulfide inhibits homocysteine-induced endoplasmic reticulum stress and neuronal apoptosis in rat

hippocampus via upregulation of the BDNF-TrkB pathway. Acta Pharmacol Sin 2014; 35: 707-715.

[24] Yang X, Xu H, Hao Y, Zhao L, Cai X, Tian J, Zhang M, Han X, Ma S, Cao J, Jiang Y. Endoplasmic reticulum oxidoreductin 1α mediates hepatic endoplasmic reticulum stress in homocysteine-induced atherosclerosis. Acta Biochim Biophys Sin (Shanghai) 2014; 46: 902-910.

[25] Hsia TC, Liu WH, Qiu WW, Luo J, Yin MC. Maslinic Acid Induces Mitochondrial Apoptosis and Suppresses HIF-1α Expression in A549 Lung Cancer Cells under Normoxic and Hypoxic Conditions. Molecules 2014; 19: 19892-19906.

[26] Maroni P, Matteucci E, Drago L, Banfi G, Bendinelli P, Desiderio MA. Hypoxia induced E-cadherin involving regulators of Hippo pathway due to HIF-1α stabilization/nuclear translocation in bone metastasis from breast carcinoma. Exp Cell Res 2014; 330: 287-299.